

Full Configuration Interaction Excitations of Ethene and Butadiene: Resolution of an Ancient Question

Csaba Daday,[†] Simon Smart,[‡] George H. Booth,[‡] Ali Alavi,^{*,‡} and Claudia Filippi^{*,†}

[†]MESA+ Institute for Nanotechnology, University of Twente, P.O. Box 217, 7500 AE Enschede, The Netherlands

[‡]University of Cambridge, Chemistry Department, Lensfield Road, Cambridge CB2 1EW, United Kingdom

S Supporting Information

ABSTRACT: We employ the recently developed full configuration interaction quantum Monte Carlo (FCIQMC) method to compute the $\pi \rightarrow \pi^*$ vertical excitation energies of ethene and all-*trans* butadiene. These excitations have been the subject of extensive theoretical studies, and their location with respect to the corresponding absorption band maximum is the source of a long lingering debate. Here, we reliably estimate the vertical excitations of ethene and butadiene by performing FCIQMC calculations for spaces as large as 10^{18} and 10^{29} Slater determinants, respectively. For ethene, we obtain a vertical excitation energy in the range 7.89–7.96 eV, depending on the particular equilibrium ground-state geometry employed, and definitely higher than the absorption maximum located at 7.66 eV. For the computationally more challenging case of butadiene, our calculations provide a robust estimate of about 6.3 eV for this excitation, that is, 0.4 eV higher than the corresponding absorption band maximum. Our FCIQMC excitation energies represent a reliable benchmarking reference for future calculations.

1. INTRODUCTION

The $\pi \rightarrow \pi^*$ vertical excitation energies of ethene and all-*trans* butadiene have been the subject of a remarkably large number of theoretical investigations.^{1–24} A wide variety of ab initio methods has been employed, but little consensus has been reached on the exact location of the vertical excitations to the 1^1B_{1u} and 1^1B_u states of ethene and butadiene, respectively. Importantly, despite the evident difficulty of obtaining a reliable estimate of their excitation energies, ethene and butadiene are often chosen as test cases to assess the accuracy of theoretical approaches for excited states.^{3,5,11,12,14,24}

Experimentally, the absorption spectrum of ethene in the far ultraviolet region consists of a broad continuous band with a maximum at 7.66 eV.^{25,26} A direct comparison between the experimental absorption maximum and the computed vertical excitation energy is meaningful if the transition probability is largest at the ground-state minimum. Since the Franck–Condon envelope might be significantly distorted for the active 1^1B_{1u} state of ethene, an excitation energy of 7.8 eV was estimated based on an intensity weighted average energy calculated from the experimental spectrum.⁶ Moreover, an earlier theoretical study indicated that nonadiabatic effects should also be taken in account, which will lead to a further blue shift in the location of the vertical excitation with respect to the band maximum.¹ Several attempts to directly compute the full spectrum have unfortunately not clarified the issue since qualitative agreement in the description of the intensity distribution has been obtained with rather different theoretical models, for instance, either discarding or including nonadiabatic couplings to other electronic excited states.^{1,9,10,27}

Most calculations of the 1^1B_{1u} vertical excitation of ethene obtain values higher than the experimental absorption maximum. The most reliable complete-active-space second-order perturbation theory (CASPT2) estimates lie between 7.8 and 8.0 eV,^{5,12,15} and coupled cluster (CC) approaches up to

perturbative third order place the excitation in the same energy range.^{4,9,12} In contrast, two investigations^{7,13} obtain a vertical excitation energy of the order of 7.7 eV, that is, very close to the experimental absorption maximum at 7.66 eV and therefore exclude a significant impact of nonadiabatic vibronic effects on the location of the absorption maximum. These calculations employ multireference coupled-cluster and configuration-interaction approaches on appropriately constructed molecular orbitals⁷ or multireference perturbation approaches on orbitals obtained with restricted active space methods.¹³ The difficulty in computing the $\pi \rightarrow \pi^*$ vertical excitation energy of ethene is evident from the spread of theoretical estimates, and is generally attributed to the so-called valence–Rydberg mixing, namely, the presence of a Rydberg-like state close in energy to the excited state of interest, which is instead essentially valence in nature. Unless electron correlation is accurately described, the Rydberg state might undesirably mix in, rendering the resulting wave function unduly diffuse and its energy unreliable. A recent study comparing the many different computed values in the literature¹² concludes that “the vertical excitation energy of the 1^1B_{1u} state can still not be assigned precisely, but should lie between 7.7 and 8.0 eV”.

For butadiene, the situation is equally confused. The 1^1B_u state has been experimentally investigated by electron impact and optical spectroscopy, and the absorption spectrum is characterized by broad bands between 5.7 and 6.3 eV, with the intensity maximum at 5.92 eV.^{28–30} Similarly to the case of ethene, the vertical excitation energy is believed to be blue-shifted with respect to this value. Theoretically, valence–Rydberg mixing represents a problem also for the description of the valence 1^1B_u state of butadiene and a rather large spread of computational estimates can in fact be found in the literature.

Received: June 12, 2012

Available CASPT2 calculations give excitation energies in the range 6.1–6.3 eV,^{3,14,18} but these single-state studies are hard to compare as they employ different zero-order Hamiltonians^{14,18} or, in the presence of diffuse functions, lead to a too diffuse state due to the lack of a multistate treatment of the close Rydberg state.³ Various flavors of CC calculations yield values between 6.2 and 6.4 eV.^{4,17,22,23} A recent multireference coupled cluster study obtains an excitation energy of 6.18 eV²⁰ with the use of molecular orbitals constructed with a similar procedure to the one adopted by the same group for ethene.⁷

Here, we employ the recently developed full configuration interaction quantum Monte Carlo (FCIQMC) method^{31–35} to compute the bright $\pi \rightarrow \pi^*$ excitations of ethene and all-*trans* butadiene. While a conventional full configuration interaction (FCI) calculation would not be feasible for these systems, the FCIQMC approach offers a computationally costly but practical route to obtain the FCI limit of these excitation energies with several orders of magnitude less memory requirements. We recall that the largest reported FCI calculation has been performed for the nitrogen molecule and a space of 10^{10} Slater determinants.³⁶ In contrast, we treat here FCI spaces of 10^{18} determinants for ethene and 10^{29} determinants for butadiene corresponding to a partially augmented triple-valence basis and a partial triple-valence basis, respectively.

The article is organized as follows. In Section 2, we give a short description of the FCIQMC method and summarize the aspects specific to the current calculations. In Section 3, we present our choice of basis sets and geometries. In Section 4, we discuss our results and compare them with previous calculations in the literature. Section 5 summarizes our conclusions.

2. THE FCIQMC METHOD

The recently developed FCIQMC approach yields the FCI solution of the Schrödinger equation stochastically and with significantly less memory requirements than conventional FCI.^{31–35} The method is based on the formulation of projection Monte Carlo in Slater determinant space, so the ground-state wave function is obtained as

$$\Psi_0 = \lim_{\tau \rightarrow \infty} e^{-\tau(\mathcal{H}-E)}\Psi^{(0)} \quad (1)$$

where the trial energy E is adjusted to the value of the ground-state energy and $\Psi^{(0)}$ is some initial wave function. If we express the wave function in the basis of Slater determinants, D_i , generated by arranging the electrons in a given set of spin orbitals, we obtain the FCI representation of the wave function,

$$\Psi = \sum_i c_i D_i \quad (2)$$

The projection (eq 1) formulated in this determinantal basis is then equivalent to a set of coupled equations for the evolution of the determinant coefficients in the CI expansion as

$$-\frac{dc_i}{d\tau} = (H_{ii} - E)c_i + \sum_{j \neq i} H_{ij}c_j \quad (3)$$

where H_{ij} are the matrix elements of the Hamiltonian between the Slater determinants.

The evolution of the CI coefficients is simulated through the dynamics of a population of N_w walkers, which are distributed over the determinants and can carry a positive or a negative sign. The parameter τ is discretized, and the walkers evolve

according to the terms in eq 3: Walkers can spawn new walkers onto other determinants (off-diagonal terms), and each walker can die or clone (diagonal term), depending on the trial energy, which is varied to keep the population roughly constant at a target value. After every step, walkers of opposite sign on the same determinant annihilate each other to ensure sign coherence.^{31,37} While the algorithm still scales exponentially with the system size, FCIQMC achieves convergence to the FCI limit with populations of walkers that are a fraction of the dimensions of the determinant space (N_{FCI}) as demonstrated for systems with spaces ranging from 10^9 to 10^{14} determinants.³¹ The gain with respect to a conventional FCI simulation is system dependent and rather hard to predict, being for instance minor in the relatively simple case of methane and significant for other notoriously difficult molecules.

A dramatic improvement to this original formulation is represented by the so-called initiator approach,³² which significantly reduces the population needed and extends the applicability of FCIQMC to more complex systems and larger basis sets.^{32–35} In the initiator approach, spawning to empty determinants is only allowed from determinants, dubbed “initiators”, with a number of walkers exceeding a certain threshold, n_{add} . Except for the special case of “double-spawning”, the progeny of noninitiator determinants survive only if they are spawned onto an already occupied determinant. Double-spawning occurs if two noninitiators simultaneously spawn walkers onto the same (originally empty) determinant: If the two progeny are of the same sign, they are allowed to survive. Such double-spawning events are rare but are found to be helpful in establishing sign coherence.³² Clearly, the initiator algorithm reduces to the FCIQMC algorithm in the limit of a large number of walkers, since in this limit, all determinants acquire an occupancy, and therefore, walkers spawned from noninitiators will survive as per the original FCIQMC algorithm. In practice, the convergence of the correlation energy with walker number to the FCI result is very rapid and occurs well before all determinants have acquired an occupation. It does, however, have a system dependence: Generally speaking, weakly correlated systems will converge more rapidly with walker number than strongly correlated ones. The standard protocol of an initiator-FCIQMC simulation is to perform calculations with increasing numbers of walkers, and to monitor the convergence of the energy. It is found that the initiator-FCIQMC method is still characterized by exponential scaling, but the exponent is now significantly smaller than with FCIQMC. In other words, the relation between the size of the walker population and dimension of the FCI space is given by

$$N_w \propto (N_{\text{FCI}})^\alpha \quad (4)$$

but the initiator approach significantly reduces the value of α with respect to the original FCIQMC algorithm, characterized by walker populations roughly linear with the FCI size, $\alpha \approx 1$.³¹ For calculations with the initiator approach, values of α between 0.16 for neutral and ionized atoms up to sodium³⁴ and 0.34 for C_2 ³⁵ have been reported.

Here, we employ the initiator variant of the FCIQMC method and report below the value of n_{add} used in each calculation. We construct the Slater determinants from the Hartree–Fock orbitals and expand the wave functions on spin-flip combinations of determinants constructed to exclude odd-spin states.³⁵ This is particularly relevant for the computation of the 1^1B_{1u} and 1^1B_u excited states of ethene and butadiene, respectively, because it ensures that the solution converges to

the singlet state of the chosen spatial symmetry and not to the triplet state, which is lower in energy. While even-spin states other than the singlet are not excluded, they are significantly higher in energy and therefore projected out in the dynamics. All simulations are started from one walker on the reference configuration state function, which is the Hartree–Fock determinant in the ground-state calculations and a spin-flip combination for the excited states. We grow the walker population to a target value while keeping the trial energy fixed to the Hartree–Fock value, and then release the trial energy into variable mode to maintain the population stationary. The energy is computed with the so-called mixed estimator as

$$E_{\text{proj}} = \frac{\langle D_0 | \mathcal{H} | \Psi_{\text{FCI}} \rangle}{\langle D_0 | \Psi_{\text{FCI}} \rangle} = \sum_j \langle D_0 | \mathcal{H} | D_j \rangle \frac{\langle N_j \rangle}{\langle N_0 \rangle} \quad (5)$$

where the coefficient c_i in the expansion is estimated as the average of the sum, N_i , of the signs of all walkers on that determinant. In this energy expression, we still denote with D_i the corresponding spin-flip combination of determinants.

3. COMPUTATIONAL DETAILS

All FCIQMC calculations are performed with the Alavi group code (NECI) and the setup of the one- and two-electron integrals and molecular orbitals necessary for FCIQMC is carried out with the Q-Chem code.³⁸ We employ the frozen-core approximation and keep the molecular orbitals corresponding to the 1s electrons of the carbon atoms doubly occupied. This amounts to freezing 4 and 8 spin-orbitals for ethene and butadiene, respectively.

The ground-state equilibrium structures are optimized at the MP2 level with the Gaussian 09 code³⁹ and at the CASPT2 level with the MOLCAS code version 7.4.⁴⁰ We investigate the basis-set dependence of the excitation energies within linear response coupled-cluster (CC) theory^{41,42} at the singles and doubles (CCSD)⁴³ and approximate third (CC3)^{44,45} orders, using the Dalton 2.0 program.⁴⁶ We also perform equation-of-motion coupled cluster calculations at the singles, doubles, and triples (EOM-CCSDT) order^{47,48} using the CFOUR program, version 1.0.⁴⁹ The frozen-core approximation is employed in the CC calculations.

3.1. Choice of Basis Sets. To optimize the ground-state equilibrium structures and investigate their basis set dependence, we employ the Dunning's correlation consistent cc-pVXZ basis sets.⁵⁰ For the computation of the excitation energies, we use the ANO-L-VXZP basis sets⁵¹ with the following contraction scheme: ANO-L-VDZP [3s2p1d]/[2s1p], ANO-L-VTZP [4s3p2d1f]/[3s2p1d], ANO-L-VQZP [5s4p3d2f]/[4s3p2d], and ANO-L-V5ZP [6s5p4d3f]/[5s4p3d].

In Table 1, we detail how we augment the ANO-L-VXZP basis sets with the diffuse functions from the corresponding aug-cc-pVXZ and d-aug-cc-pVXZ basis sets,⁵² and how we label the various augmented basis sets. For example, in the VDZP+C(p) set, we only augment the basis on the C atoms with the diffuse *p* function from the aug-cc-pVDZ basis while we use the full augmentation on the C atoms in the VDZP+C basis set. In the VDZP+double basis set, the augmentation from the d-aug-cc-pVDZ is employed on the C atoms in combination with the augmentation from the aug-cc-pVDZ on the H atoms. Finally, we also construct a VTZP' basis set without augmentation, where the VTZP basis set without *f*-functions is employed on the carbon atoms, and the VDZP basis set on the hydrogen atoms.

Table 1. Number and Type of Diffuse Functions Employed to Augment the ANO-L-VXZP Basis Sets on the Carbon (Aug-C) and Hydrogen (Aug-H) Atoms^a

basis	label	aug-C	aug-H
ANO-L-VDZP	+C(p)	1p	
	+C	1s1p1d	
	+all	1s1p1d	1s1p
	+double	2s2p2d	1s1p
ANO-L-VTZP'			
ANO-L-VTZP	+C(s,p,d)	1s1p1d	
	+all	1s1p1d1f	1s1p1d
	+double	2s2p2d2f	1s1p1d
ANO-L-VQZP			
	+C	1s1p1d1f	
	+all	1s1p1d1f	1s1p1d

^aThe label we assign to the resulting augmented basis set is also listed.

3.2. Ground-State Equilibrium Geometries. Previous calculations of the vertical excitation energies of ethene and all-*trans* butadiene have been performed on a variety of geometrical models either optimized with different ab initio methods or from different experimental studies. For butadiene, in particular, there are at least four different structures derived from independent experimental data,^{53–56} which give a spread of about 0.012 Å in the carbon–carbon double bond, well outside the reported error bars, as shown in Table 2. For ethene, most previous calculations of the vertical excitation energy have employed the geometry from the experimental study of ref 57, but it is worth noting that another structure has been reported with a carbon–carbon bond length not compatible within the given error bar⁵⁸ (see Table 2). Given the uncertainty in the structures derived from experiments, we generate here the ground-state equilibrium structures with the MP2 method and validate our choice against CASPT2 geometries.

We optimize the MP2 geometries with cc-pVXZ basis set series and list the carbon–carbon bond lengths in Table 2. We impose D_{2h} symmetry for ethene and C_{2h} symmetry for butadiene, and place ethene in the *yz*-plane along the *z*-axis, so the $\pi \rightarrow \pi^*$ excited state has B_{1u} symmetry. We find that the cc-pVQZ basis set gives converged bond lengths to better than 0.001 Å, while smaller basis sets yield slightly elongated bond lengths with a discrepancy of about 0.015 Å for the smallest cc-pVDZ basis set. To assess the quality of the MP2/cc-pVQZ geometries, we also optimize the structures with the CASPT2/cc-pVQZ method. We use a CAS(2,2) and a CAS(4,4) expansion for ethene and butadiene, respectively, where all π electrons in the reference are correlated in an equal number of π orbitals. For ethene, we also consider the larger CAS(6,6) active space where σ and π electrons are correlated over the orbitals ($1b_{2g}$, $1b_{3u}$, $3a_g$, $1b_{3g}$, $2b_{2u}$, $3b_{1u}$) as in ref 7. The differences between the CASPT2 and MP2 bond lengths optimized with the same cc-pVQZ basis are smaller than 0.004 and 0.002 Å in ethene and butadiene, respectively. We also note that our MP2 geometries are in excellent agreement with the equilibrium structures recently obtained by combining rotational spectroscopic data with vibration–rotation constants from quantum chemical calculations⁵⁹ (denoted with “semi-exp” in Table 2).

Table 2. Carbon–Carbon Bond Lengths (Å) of Ethene and Butadiene Optimized with the MP2 and CASPT2 Methods and the cc-pVXZ Basis Set with X = D, T, Q, 5^a

molecule	method	basis	C=C	C–C	ΔE (eV)
ethene	MP2	D	1.346		7.95
	MP2	T	1.332		8.05
	MP2	Q	1.330		8.06
	MP2	S	1.329		8.07
	CASPT2/CAS(2,2)	Q	1.332		8.05
	CASPT2/CAS(6,6)	Q	1.333		8.04
	exp ⁵⁷		1.339		8.00
	exp ⁵⁸		1.334(1)		8.03
	semi-exp ⁵⁹		1.3305(10)		8.06
butadiene	MP2	D	1.353	1.464	6.27
	MP2	T	1.340	1.453	6.35
	MP2	Q	1.338	1.451	6.36
	MP2	S	1.338	1.450	6.36
	CASPT2/CAS(4,4)	Q	1.340	1.452	6.35
	exp ⁵³		1.343(9)	1.467(2)	6.36
	exp ⁵⁴		1.341(2)	1.463(3)	6.36
	exp ⁵⁵		1.349(1)	1.467(2)	6.31
	exp ⁵⁶		1.337	1.467	6.40
	semi-exp ⁵⁹		1.3376(10)	1.4539(10)	6.37

^aWe also list the CCSD vertical excitation energies (eV) computed with the ANO-L-VQZP basis set for ethene, and the ANO-L-VTZP+all basis set for butadiene.

Table 3. Vertical Excitation Energies (eV) of Ethene Computed with FCIQMC on the MP2 (ΔE_{MP2}) and Experimental (ΔE_{Expt}) Geometries with Different ANO-L Basis Sets^a

basis	aug	N_{FCI}	N_w	1^1A_g		1^1B_{1u}		ΔE_{MP2}	ΔE_{Expt}
				E_{MP2}	E_{Expt}	E_{MP2}	E_{Expt}		
VDZP		5.5×10^{12}	10^6	−78.3599(1)	−78.3612(1)	−78.0538(2)	−78.0580(2)	8.33(1)	8.25(1)
	+C(p)	2.6×10^{13}	2×10^6	−78.3754(1)	−78.3762(1)	−78.0792(3)	−78.0821(3)	8.06(1)	8.00(1)
	+C	3.5×10^{14}	5×10^6	−78.3909(1)	−78.3917(1)	−78.0968(2)	−78.1001(2)	8.00(1)	7.93(1)
	+all	5.6×10^{15}	2×10^7	−78.3983(2)	−78.3987(1)	−78.1049(4)	−78.1076(4)	7.98(1)	7.92(1)
	+double	6.9×10^{16}	8×10^7	−78.4000(1)	−78.4005(1)	−78.1071(4)	−78.1103(2)	7.97(1)	7.90(1)
VTZP		4.4×10^{17}	2×10^7	−78.4370(2)	−78.4361(2)	−78.1407(3)	−78.1433(3)	8.06(1)	7.97(1)
	+C(s,p,d)	2.7×10^{18}	10^8	−78.4409(2)	−78.4410(2)	−78.1487(6)	−78.1499(6)	7.95(2)	7.92(2)

^aThe total ground- and excited-state FCIQMC energies (a.u.) are also given for both geometries together with the size of the full CI space (N_{FCI}) and the required walker population (N_w). The statistical errors on the energies are given in brackets.

We also investigate the dependence of the vertical excitation energies on the choice of geometry at the CCSD level using the ANO-L-VQZP basis for ethene and the ANO-L-VTZP+all basis set for butadiene. We find that the vertical excitation energies of both molecules are rather sensitive to relatively small changes in bond lengths. For instance, the use of MP2 geometries optimized with the cc-pVDZ basis yields excitation energies red-shifted by as much as 0.1 eV with respect to the values obtained on the MP2/cc-pV5Z structures. The excitations computed on the cc-pVQZ structures are instead converged to better than 0.01 eV. We also compute the CCSD excitations on the four experimental geometries of butadiene, where we use the available experimental parameters but the carbon–hydrogen bond lengths and HCC bond angles from the CASPT2 equilibrium geometry. The spread of 0.012 Å in the carbon–carbon double bond among the four geometries translates into variations of 0.1 eV in the computed vertical excitation energy. Clearly, the sensitivity to the choice of geometry should be taken into account when comparing theoretical studies employing different structural models of ethene and butadiene.

Having validated our choice of equilibrium geometries, we compute the FCIQMC excitation energies on the MP2/cc-pVQZ structures. This combination of method and basis has also the advantage of being easily applicable to consistently extend the present FCIQMC study to a larger set of molecules. For ethene, we also perform FCIQMC calculations on the experimental geometry from ref 57, since this geometry has been so often employed in previous theoretical studies of the same vertical excitation.

4. RESULTS

We present here the FCIQMC vertical excitation energies of ethene and butadiene computed with various basis sets. In all calculations, we use the initiator-FCIQMC approach with thresholds of $n_{\text{add}} = 3$ for ethene and $n_{\text{add}} = 5$ for butadiene. These values minimize the required size of walker populations for all basis sets in the two systems. For each basis set, the number of walkers is increased until no significant change is observed in the correlation energy. We converge the ground and excited states separately, and in general, the excited state requires more walkers for convergence. Nevertheless, we report the energies obtained with the same population size for both

states to further reduce the statistical error on the excitation energy. To estimate the remaining basis set error, we also perform CC calculations with the same basis sets as in the FCIQMC runs as well as with larger basis sets. In all the computations below, we employ the augmented ANO-L basis sets described in Table 1 and omit at times ANO-L in the acronym.

4.1. Ethene. In Table 3, we report the FCIQMC total energies of the 1^1A_g and 1^1B_{1u} states of ethene and the corresponding excitation energies. We employ the ANO double- ζ basis sets with the augmentations listed in Table 1, and the triple- ζ basis with and without +C(s,p,d) augmentation.

In all FCIQMC calculations, we find that the number of walkers needed to converge the 1^1B_{1u} state is many orders of magnitude smaller than the dimensions of the FCI space. For example, we obtain convergence with a population of approximately 10^8 walkers in a FCI space of 10^{18} determinants in correspondence of the largest VTZP+C(s,p,d) basis set. We also find that the size of the walker population scales with respect to the FCI dimension according to a power law (eq 4), as previously observed for other systems. However, as shown in Figure 1, the scaling of the augmented basis sets constructed

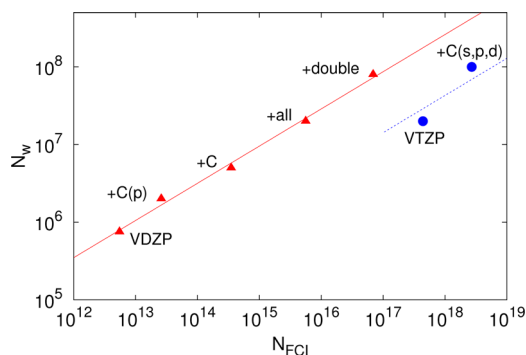


Figure 1. Logarithmic plot of the dimension of the FCI space (N_{FCI}) and the corresponding walker population (N_w) employed in the calculations of the 1^1B_{1u} state of ethene for five basis sets based on VDZP (red triangles) and two basis sets based on VTZP (blue circles). A log–log fit of the excitations computed with augmented VDZP basis sets yields a slope of $\alpha = 0.48$ (solid, red line). The blue dashed line, which is drawn with the same slope as the red line, suggests that the VTZP basis sets might display similar scaling properties.

from the ANO double- ζ basis differs significantly from that of triple- ζ basis sets. For instance, the VTZP basis set without augmentation requires the same number of walkers as the VDZP+all basis even though its FCI space is almost 100 times larger. Therefore, the triple- ζ basis sets appear to require fewer walkers than what the extrapolation from the augmented double- ζ basis sets would suggest. We believe that this difference of prefactors stems from the higher relative number of diffuse basis functions in the ANO double basis set series as compared to the two triple- ζ basis sets considered here. Indeed, once the augmentation functions are added, it is found that the π^* orbital no longer corresponds to the Hartree–Fock LUMO orbital. This potentially has significant implications regarding the rapidity of convergence of the FCI wave function of both the 1^1A_g state and the 1^1B_{1u} state, since the appearance of additional low energy determinants may result in a significantly more multiconfigurational wave function. This undesirable behavior may be ameliorated by employing a different one-electron basis, but in this study we continue to use a Hartree–Fock basis, leaving this question for a future study. In general, however, we find that the introduction of very diffuse functions leads to a slower convergence of the FCIQMC simulation. A log–log fit of only the double- ζ populations yields $\alpha = 0.48$. It is unclear from only two basis sets whether the triple- ζ basis sets have the same scaling parameter α . The scaling parameter of ethene is therefore larger than the ones obtained for first and second row atoms and anions ($\alpha = 0.16$)³⁴ or C_2 ($\alpha = 0.34$).³⁵ Clearly, the size of the FCI space is not the only relevant parameter that affects the size of the required walker population, but the relative number and the diffuseness of the augmented functions need also to be taken into account.

The FCIQMC excitation energies display a smooth convergence with respect to the basis sets of the augmented ANO double- ζ series. The VDZP+double values computed on the MP2 and the experimental geometry are equal to 7.97(1) and 7.90(1) eV, respectively, and compatible with the corresponding excitations of 7.95(2) and 7.92(2) eV obtained with the VTZP+C(s,p,d) basis set. To assess the degree of convergence of these excitation energies with basis set, we compare the FCIQMC results with the CCSD, CC3, and CCSDT excitation energies computed with much larger basis sets of up to quintuple- ζ quality.

Table 4. Vertical Excitation Energies (eV) of Ethene Calculated with CCSD, CC3, CCSDT, and FCIQMC and Different ANO-L Basis Sets on the MP2 and the Experimental Geometry (Separated by a Slash as MP2/Expt)^a

basis	aug	CCSD	CC3	CCSDT	FCIQMC
VDZP		8.44/8.37	8.33/8.26	8.34/8.26	8.33(1)/8.25(1)
	+C(p)	8.13/8.07	8.05/7.99	8.06/8.00	8.06(1)/8.00(1)
	+C	8.08/8.02	7.98/7.92	7.99/7.93	8.00(1)/7.93(1)
	+all	8.06/8.00	7.95/7.89	7.96/7.90	7.98(1)/7.92(1)
	+double	8.03/7.97	7.93/7.87	7.94/7.88	7.97(1)/7.90(1)
VTZP		8.15/8.08	8.03/7.96	8.04/7.97	8.06(1)/7.97(1)
	+C(s,p,d)	8.06/7.99	7.94/7.88	7.96/7.89	7.95(2)/7.92(2)
	+all	8.05/7.99	7.93/7.87	7.95/7.88	
	+double	8.05/7.98	7.93/7.86	7.94/7.87	
VQZP		8.06/7.99	7.94/7.88	7.96/7.89	
	+C	8.05/7.98	7.93/7.86		
	+all	8.05/7.98	7.93/7.86		
VSZP		8.05/7.99	7.93/7.87		

^aThe statistical errors on the FCIQMC excitation energies are given in brackets.

The coupled cluster excitation energies are compared with the FCIQMC values in Table 4, and the convergence of the excitations with basis set is illustrated in Figure 2. The CC3 and

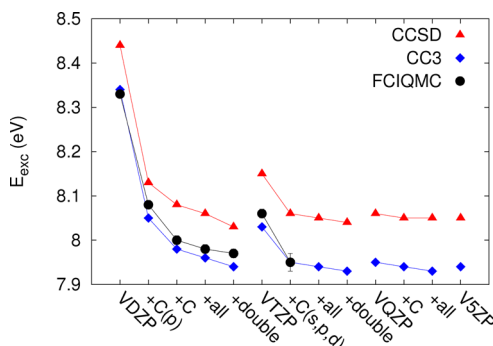


Figure 2. Basis-set convergence of the excitation energies (eV) of ethene, computed with CCSD, CC3, and FCIQMC on the MP2 geometry. A very similar behavior is observed on the experimental geometry. The statistical error bar on the FCIQMC energies is either smaller than the size of the symbols or is indicated.

CCSDT values are very close to the FCIQMC energies and the CC3 results computed with the VDZP+double and the VTZP +C(s,p,d) basis sets are converged to better than 0.01 and 0.02 eV, respectively. Given the very similar behavior of the coupled-cluster and FCIQMC excitations as a function of basis set, it is safe to expect that also the FCIQMC excitation energies computed with the VDZP+double basis set are affected by a similar, small basis-set error of at most 0.01 eV. If we correct the FCIQMC/VDZP+double values by this amount, we estimate that the vertical excitation energy of ethene is $\Delta E_{\text{MP2}} = 7.96(1)$ eV on the MP2 geometry and $\Delta E_{\text{EXP}} = 7.89(1)$ eV on the experimental geometry.

While all FCIQMC calculations have been obtained treating all possible excitations of the 12 valence electrons, it is interesting to find out which level of excitation plays an important role in our final results. Therefore, for the VDZP+all basis set that has proven to yield nearly converged results for ethene, we compute the excitation energies with excitations limited to 3, 4, 5, 6, and 8 electrons. The walker population is kept fixed at the size needed at the FCI level, namely, 2×10^7 . The 1^1A_g state is already converged with an excitation level of 5, but the 1^1B_{1u} state needs at least 6-fold excitations, as shown in Table 5.

To further validate our FCIQMC results, we investigate two possible sources of error in our calculations, that is, the frozen-

Table 5. FCIQMC Total (a.u.) and Vertical Excitation (eV) Energies of Ethene Computed with Limited Excitations^a

max exc.	1^1A_g	1^1B_{1u}	ΔE
3	-78.3700(0)	-78.0450(1)	8.84(0)
4	-78.3973(1)	-78.0948(2)	8.23(1)
5	-78.3980(1)	-78.1027(3)	8.04(1)
6	-78.3983(1)	-78.1051(3)	7.98(1)
8	-78.3983(1)	-78.1053(3)	7.97(1)
12	-78.3983(2)	-78.1049(2)	7.98(1)

^aWe employ the MP2 ground-state equilibrium geometry, the VDZP +all basis set, and a walker population of 5×10^6 . A maximum excitation (max exc.) of 12 corresponds to a (frozen-core) FCI calculation. The statistical error on the energies is given in brackets.

core approximation and the lack of additional diffuse functions. In all the FCIQMC calculations, we have frozen the lowest four orbitals corresponding to the 1s electrons of the carbon atoms. We therefore unfreeze all orbitals in the computation of the excitation energy of ethene computed with the VDZP+all basis set. As expected, the absolute ground- and excited-state energies change significantly, but the vertical excitation energy of 7.97(1) remains compatible with the value of 7.98(1) previously obtained within the frozen-core approximation, as shown in Table 6. Interestingly, while the FCI space increases by a factor of 10^4 , the required population is only 2.5 larger than in the frozen-core calculations. This can be explained with the fact that the determinants corresponding to excitations from the core have significantly higher energies and a relatively small weight, so the walker population needed to map this region of the FCI space is small relative to the total number of determinants. We note that the CCSD and CC3 excitations computed without the frozen-core approximation also change by at most 0.01 eV (see the Supporting Information).

As for the diffuseness of the basis, several previous calculations of the vertical excitation energy of ethene employ basis sets that are more diffuse than the ones considered in this work. In particular, the two investigations that have led to the lowest estimate of the vertical excitation at 7.7 eV^{7,13} have used more diffuse functions on the carbon atoms. Therefore, to verify that such diffuse functions do not change the excitation energy, we further augment our VQZP+all basis set with the p-augmentation of carbon from ref 13, by adding two sets of Gaussians with exponents 0.010727 and 0.003576 (in total, 12 additional spatial basis functions). The resulting basis set is not the same as the one used in refs 7 or 13 because ANO-L-VQZP has more primitives than cc-pVQZ, but the total number of functions is the same and the diffuse functions are identical. At the CCSD and CC3 level, we find that the additional diffuse functions have very little effect on the excitation energies which are only 0.01 eV lower than the values obtained with the VQZP +all basis.

Finally, we note that the ground-state FCIQMC energies in Table 3 should also give us an indication of the quality of the MP2 equilibrium structure as compared to the experimental geometry from ref 57. We first observe that the ground-state FCIQMC energies obtained with the VDZP basis set are lower on the experimental geometry than on the MP2 one. However, this difference diminishes as the basis is enlarged to the VDZP +double and the situation reverses at the triple- ζ level. This observation is consistent with our findings in optimizing the equilibrium geometry with different basis sets, namely, that a small basis of double valence quality favors a longer carbon-carbon bond length as the one in the experimental geometry (see Table 2). The behavior of the ground-state FCIQMC energies is similar to the one observed within CCSD, CC3, and CCSDT (see the Supporting Information).

4.2. Butadiene. For butadiene, we perform FCIQMC calculations with two basis sets without diffuse functions, namely, VDZP and VTZP', and report the total and excitation energies in Table 7. For the VDZP basis set, we obtain a converged excitation energy of 6.56(2) eV with a population of 3×10^8 walkers, and further increasing the population to 10^9 walkers leads to a ground-state energy compatible within statistical error and only a slightly lower excited-state energy, reducing the excitation energy to 6.53(2) eV. The VTZP' basis yields a FCI space of 10^{29} determinants and requires instead populations of at least 10^9 walkers, which is computationally

Table 6. FCIQMC Total (E in a.u.) and Vertical Excitation (ΔE in eV) Energies of Ethene Computed with and without Frozen Orbitals^a

orb. frozen	N_{FCI}	N_w	$E(1^1A_g)$	$E(1^1B_u)$	ΔE
0	7.9×10^{19}	5×10^7	-78.4121(1)	-78.1193(2)	7.97(1)
4	5.6×10^{15}	2×10^7	-78.3983(2)	-78.1049(2)	7.98(1)

^aThe VDZP+all basis set and the MP2 equilibrium geometry are used. The statistical error on the energies is given in brackets.

Table 7. Vertical Excitation Energies (ΔE in eV) of Butadiene Computed with FCIQMC with Different ANO-L Basis Sets^a

basis	N_{FCI}	N_w	$E(1^1A_g)$	$E(1^1B_u)$	ΔE
VDZP	2.5×10^{25}	3×10^8	-155.5481(6)	-155.3072(4)	6.56(2)
		10^9	-155.5491(4)	-155.3092(6)	6.53(2)
VTZP'	1.1×10^{29}	10^9	-155.6076(4)	-155.373(1)	6.38(3)

^aThe total ground- and excited-state FCIQMC energies (a.u.) are also given together with the size of the full CI space (N_{FCI}) and the required walker population (N_w). The statistical error on the energies is given in brackets.

quite demanding and at the limits of what we can afford. With this population size, we achieve convergence for the ground-state energy but cannot further increase the number of walkers to verify convergence of the excited state.

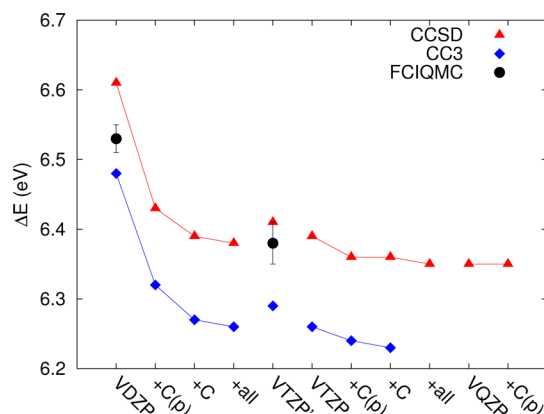
Nevertheless, we believe that the corresponding VTZP' excitation energy of 6.38(3) eV is nearly converged to the FCI limit for two reasons. First, halving the number of walkers yields a compatible ground-state energy within a statistical error of 1 mHartree and raises the excited-state energy by less than 3 ± 1 mHartree. The corresponding excitation energy is increased by 0.10 ± 0.05 eV. The convergence behavior for the two basis sets without diffuse functions in ethene and for the VDZP basis in butadiene reveals that the excited state requires a walker population less or equal to roughly twice the population needed for the ground state. Since we obtain convergence for the ground state of butadiene in the VTZP' basis set with 5×10^8 walkers, we do not expect that a further increase of the population beyond 10^9 for the excited state will significantly affect the excitation energy. Second, we can assess convergence of our FCIQMC total and excitation energies through a comparison with the CCSD, CC3, and CCSDT values. As shown in Table 8 and in Figure 3, our FCIQMC

Table 8. Vertical Excitation Energies (eV) of Butadiene Calculated with Coupled Cluster and FCIQMC^a

basis	aug	CCSD	CC3	CCSDT	FCIQMC
VDZP		6.61	6.48	6.50	6.53(2)
	+C(p)	6.43	6.32	6.34	
	+C	6.39	6.27	6.29	
	+all	6.38	6.26	6.27	
VTZP'		6.41	6.29	6.31	6.38(3)
VTZP		6.39	6.26	6.28	
	+C(p)	6.36	6.24	6.25	
	+C(s,p,d)	6.36	6.23		
	+all	6.35			
VQZP		6.35			
	+C(p)	6.35			

^aThe statistical error on the energies is given in brackets.

excitation energies appear to have a similar convergence behavior as the CC values. For both basis sets, they lie in the range bordered on the high side by the CCSD and on the low side by the CCSDT or CC3 values, being slightly closer to CCSD. The difference of 0.15 eV between the FCIQMC excitation energies computed with the two basis sets is rather

**Figure 3.** Basis-set convergence of the vertical excitation energies (eV) of butadiene, computed with CCSD, CC3, and FCIQMC.

comparable to what is obtained within CC. Furthermore, if we compare the total ground- and excited-state FCIQMC energies with the corresponding frozen-core CCSD values (see the Supporting Information), we find that FCIQMC gives very similar shifts with respect to CC for both VDZP and VTZP' basis sets. These facts lead us to conclude that the employed walker population of 10^9 is close to sufficient for the VTZP' basis set.

To estimate the remaining basis set error, we note that the CC results are converged when the VTZP+C(p) and larger basis sets are employed, and that VTZP' yields CC excitations which are only 0.06 eV higher than the converged values. Given the similar convergence behavior of FCIQMC, we expect that the basis-set correction should not be significantly different from the 0.06 eV value estimated within CC. With the use of this correction, we assign a value of $\Delta E = 6.32(3)$ eV to the vertical excitation of butadiene.

Finally, we note that, as in the case of ethene, the use of basis sets with diffuse functions slows down the convergence of the FCIQMC energies and leads to even larger walker populations, especially for the 1^1B_u state. For instance, even though the VDZP+C and VTZP' basis sets are characterized by exactly the same size of FCI space, the excited state shows a significantly slower convergence with population size for the VDZP+C basis. In particular, the VDZP+C excited-state energy computed with a population of 10^9 walkers is significantly closer to the CCSD value than what is observed for the VDZP and VTZP' basis sets, and therefore too high (see the Supporting Information).

Table 9. Vertical Excitation Energies (ΔE in eV) of Ethene from the Literature^a

method	basis	total augmentation			C=C	ΔE	ref
		C	H	center			
MR-AQCC	aug-cc-pVQZ	1s3p1d ^b			1.339	7.69	7
MR-CISD+Q	aug-cc-pVQZ	1s3p1d ^b			1.339	7.69	7
RASSCF/NEVPT2	aug-cc-pVQZ	1s3p1d	1s1p1d		1.339	7.65–7.75	13
RASSCF/CASPT2	aug-cc-pVQZ	1s3p1d	1s1p1d		1.339	7.70–7.80	13
CCSD	ANO-L [4s3p2d]/[3s2p]	2s2p1d			1.339	7.98	4
CCSD(T)	ANO-L [4s3p2d]/[3s2p]	2s2p1d			1.339	7.99	4
CCSDT-3	ANO-L [4s3p2d]/[3s2p]	2s2p1d			1.339	7.89	4
CC3	d-aug-cc-pVQZ	2s2p2d2f	2s2p2d2f		1.336	7.88	12
MS-CASPT2	d-aug-cc-pV5Z	2s2p2d2f	2s2p2d2f		1.336	7.83	12
MS-CASPT2	ANO-L [5s4p2d]/[3s2p]			1s1p1d	1.336	7.98	5
MS-CASPT2	ANO-L [4s3p1d]/[2s1p]			1s1p1d	1.339	8.04	15
MS-RASPT2	ANO-L [4s3p1d]/[2s1p]			1s1p1d	1.339	8.13	15
CCSD	ANO-L-VQZP+all	1s1p1d1f	1s1p1d		1.339	7.98	this work ^c
CC3	ANO-L-VQZP+all	1s1p1d1f	1s1p1d		1.339	7.86	this work ^c
CCSDT	ANO-L-VTZP+double	2s2p2d2f	1s1p1d		1.339	7.87	this work ^c
FCIQMC	ANO-L-VDZP+double	2s2p2d			1.339	7.90(1)	this work ^{c,d}
FCIQMC	basis-set-corrected				1.339	7.89(1)	this work ^c
FCIQMC	ANO-L-VDZP+double	2s2p2d			1.330	7.97(1)	this work ^{e,f}
FCIQMC	basis-set-corrected				1.330	7.96(1)	this work ^e
exp						7.66	25, 26 ^g
exp						7.8	6 ^h

^aWe list the employed basis sets (basis name and number of diffuse functions on the carbon and hydrogen atoms, and centered on the molecule) and the carbon–carbon bond length (Å). For each paper, we report the excitation energy computed with the largest basis set considered. ^bOnly the z component of two most diffuse p augmentation functions is included. ^cExperimental geometry from ref 57. ^dThe ANO-L-VTZP+C(s,p,d) basis yields a compatible value of 7.92(2) eV. ^eMP2/cc-pVQZ equilibrium geometry (this work). ^fThe ANO-L-VTZP+C(s,p,d) basis yields a compatible value of 7.95(2) eV. ^gUV absorption maximum. ^hWeighted average energy from the UV absorption spectrum.

Table 10. Vertical Excitation Energies (ΔE in eV) of Butadiene from the Literature^a

method	basis ^b	total augmentation			C=C	C–C	ΔE	ref
		C	H					
MR-AQCC	aug-cc-pVTZ	2s2p1d	1s1p		1.343	1.467	6.18	20
MR-CISD+Q	aug-cc-pVTZ	2s2p1d	1s1p		1.343	1.467	6.34	20
CCSD	ANO-L [6s3p1d]/[2s1p]	2p			1.343	1.467	6.42	4
CCSD(T)	ANO-L [6s3p1d]/[2s1p]	2p			1.343	1.467	6.36	4
CCSD	aug-cc-pVTZ	1s1p1d1f	1s1p1d		1.340	1.454	6.35	22
CCSDR(3)	aug-cc-pVTZ	1s1p1d1f	1s1p1d		1.340	1.454	6.21	22
CC3	aug-cc-pVTZ	1s1p1d1f	1s1p1d		1.340	1.454	6.20	22
SS-CASPT2	ANO-L [6s3p1d]/[2s1p]	2p			1.343	1.467	6.23	3
SS-CASPT2	ANO-L-VDZP				1.347	1.466	6.06	18
SS-CASPT2	ANO-L [4s3p2d]/[2s1p]				1.354	1.458	6.29	14
SS-RASPT2	ANO-L [4s3p2d]/[2s1p]				1.354	1.458	6.31	14
SAC–CI	DZP [4s2p1d]/[2s]	4s4p2d			1.340	1.465	6.33	21
CCSD	ANO-L-VQZP+C(p)	1p			1.338	1.451	6.36	this work
CC3	ANO-L-VTZP+C(s,p,d)	1s1p1d			1.338	1.451	6.23	this work
CCSDT	ANO-L-VTZP+C(p)	1p			1.338	1.451	6.25	this work
FCIQMC	ANO-L [4s3p2d]/[2s1p]				1.338	1.451	6.38(3)	this work
FCIQMC	basis-set-corrected				1.338	1.451	6.32(3)	this work
exp							5.92	28–30 ^c
exp							5.95–6.00	28 ^d

^aWe list the employed basis sets (basis name and number of diffuse functions on the carbon and hydrogen atoms) and the carbon–carbon bond length (Å). For each paper, we report the excitation energy computed with the largest basis set considered. ^bLargest basis in a given article. ^cExperimental value from optical^{28,30} or electron impact spectroscopy.²⁹ ^dWeighted average energy from the UV absorption spectrum.

4.3. Theoretical Comparison. In Table 9, we collect the most relevant calculations of the vertical excitation energy of ethene from the literature, and compare them with our FCIQMC estimates of 7.96(1) and 7.89(1) eV on the MP2/cc-pVQZ and the experimental geometry of ref 57, respectively.

We note that the listed calculations have been performed mainly on the same experimental geometry or on a geometry characterized by a carbon–carbon bond length between our MP2 (1.330 Å) and the experimental value (1.339 Å). Therefore, these calculations can be either directly compared

with our FCIQMC excitation on the same experimental structure or with a reference value, which should lie between the FCIQMC estimates of 7.89(1) and 7.96(1) eV obtained on the experimental and MP2 structures. Multistate (MS) CASPT2 calculations^{5,12,15} and previous CC calculations up to perturbative third order^{4,12} give excitations in the range 7.8–8.0 eV. At variance with these calculations, an excitation energy of 7.7 eV is obtained with either multireference (MR) configuration interaction and coupled cluster methods on appropriately constructed molecular orbitals,⁷ or with the perturbative NEVPT2 approach with the use of orbitals obtained with restricted active space methods.¹³ Therefore, the CASPT2 and CC results are compatible with our FCIQMC excitation energies, while the value of 7.7 eV reported in refs 7 and 13 is significantly lower. We reiterate that this difference does not stem from the choice of geometry since we employ the same experimental structure, nor from the use of more diffuse augmented functions, which only affects the excitation energy by 0.01 eV, as shown. It is rather difficult to establish why refs 7 and 13 obtain such a low excitation. In our FCIQMC calculations, there is no need to artificially constrain the available excitations to an appropriate set of orbitals as in the RASSCF and subsequent NEVPT2 calculations of ref 13 and size-extensivity is guaranteed, unlike the MR-CISD+Q calculations of ref 7, which are based on the Davidson correction⁶⁰ on CISD values. In fact, bare MR-CISD with the largest CAS reference gives an excitation energy of 7.57 eV, which means that a Davidson correction of 0.12 eV is significant and that the excitation energy is likely to become larger when higher excitations are included in the CI expansion.

Table 10 reports a similar comparison for the vertical excitation energy of butadiene. Several calculations in the literature compare rather well with our FCIQMC estimate of 6.32(3) eV. Previous CC calculations yield excitation energies in the range 6.2–6.4 eV^{4,22} with CC3 and CCSD being at the low and the high side of this range, respectively. The single-state (SS) CASPT2 and RASPT2 excitation energies of about 6.3 eV¹⁴ are in good agreement with our FCIQMC estimate, while the CASPT2 value of 6.0 eV¹⁸ is significantly red-shifted, possibly due to the use of a different zero-order Hamiltonian. It is hard to establish the quality of the CASPT2 calculation of ref 3 due to the lack of multistate treatment in combination with the use of diffuse functions, which induce valence–Rydberg mixing in the excited state. The MR-CISD+Q result of 6.34 eV²⁰ is also in very good agreement with our FCIQMC excitation energy, but their MR-AQCC value of 6.18 eV is too red-shifted. In comparing the excitation energies of Table 10, we must however, keep in mind that they are computed with different geometries and basis sets and that the quality of the basis sets is less uniform than in the previous comparison for ethene. For instance, our CC calculations show that the VDZP basis employed in ref 18 is clearly inadequate. On the other hand, we expect that the geometrical differences affect to a lesser degree the corresponding vertical excitations. From Table 2, we can see for example that our MP2/cc-pVQZ geometry gives the same excitation energy at the CCSD level as the experimental geometry⁵³ employed in refs 3 and 4. Similarly, our CC results agree within 0.01–0.04 eV with the ones of ref 22, where yet another geometry, optimized with the MP2 method but with a TZ-VPP basis set, is used.

Finally, we compute a weighted average value of the absorption spectrum of butadiene,²⁸ namely, $\int I \, dE / \int (I/E) \, dE$, as proposed in ref 6 for ethene, and obtain a value of

5.95–6.00 eV, depending on the limits of integration. This estimate is a better estimate of the vertical excitation than the band maximum because it takes into account adiabatic Franck–Condon coupling. However, it is still significantly lower than our FCIQMC excitation energy and most other values in the literature, indicating that nonadiabatic couplings to other excited states are important.

5. CONCLUSIONS

In this work, we employ the recently developed FCIQMC method to compute the $\pi \rightarrow \pi^*$ vertical excitation energies of ethene and butadiene, which have been the subject of extensive theoretical investigation for more than two decades and for which reliable estimates are still needed. For this complex problem, FCIQMC allows us to treat remarkably large FCI spaces, which would be unthinkable for conventional FCI, namely, 10^{18} determinants for ethene and 10^{29} determinants for butadiene corresponding to a partially augmented triple-valence basis and a partial triple-valence basis, respectively.

For ethene, we obtain a vertical excitation energy in the range 7.89–7.96 eV, depending on the particular equilibrium ground-state geometry employed. These values correspond to the FCIQMC limit for a double-augmented ANO-L basis set of double- ζ quality corrected for a basis-set error of 0.01 eV estimated within CC. The analysis of the FCIQMC excitations computed with a series of basis sets up to a partially augmented ANO-L triple-valence basis confirms our extrapolation. The vertical excitation energy is therefore definitely higher than the experimental absorption band maximum located at 7.66 eV, indicating that nonadiabatic effects are important and responsible for shifting the location of the vertical excitation to higher energies. For butadiene, the FCIQMC computation of the excitation is significantly more challenging even though the approach is able to reduce the complexity of the problem by 12 orders of magnitude, with respect to conventional FCI. With an ANO-L triple-valence basis on the carbon atoms, we are close to convergence to the FCIQMC limit with populations of 10^9 walkers, but going to larger populations is currently beyond our computational possibilities. Our best estimate is a vertical excitation of about 6.3 eV, which we obtain with the use of a partial ANO-L triple-valence basis and a basis-set correction of 0.06 eV estimated within CC. This value is significantly blue-shifted with respect to the location of the absorption band maximum at 5.92 eV, indicating the importance of nonadiabatic effects also in butadiene. Our recommended estimates of the vertical excitation energies of both molecules represent a robust, reliable benchmarking reference for future calculations.

■ ASSOCIATED CONTENT

Supporting Information

Ground-state geometries of ethene and butadiene. Convergence of the MP2 geometry of ethene with various basis sets. Ground-state coupled-cluster energies of ethene and butadiene computed with the ANO basis sets. Excitation energies of ethene computed with CCSD and CC3 without the frozen-core approximation. This information is available free of charge via the Internet at <http://pubs.acs.org/>.

■ AUTHOR INFORMATION

Corresponding Author

*E-mail: asa10@cam.ac.uk; c.filippi@utwente.nl.

Notes

The authors declare no competing financial interest.

■ ACKNOWLEDGMENTS

C.D. is supported by NWO/CW (ECHO Grant No. 712.011.005). A.A. is supported by the Engineering and Physical Sciences Research Council of the U.K. (Grant No. EP/J0038671/1). We acknowledge the support of the Donald Smit Center for Information Technology, University of Groningen, for the use of their Blue Gene machine (<http://www.rug.nl/cit/hpcv/faciliteiten/BlueGene>). This work made use of the facilities of HECToR, the U.K.'s national high-performance computing service, which is provided by UoE HPCx Ltd at the University of Edinburgh, Cray Inc and NAG Ltd, and funded by the Office of Science and Technology through EPSRC's High End Computing Programme.

■ REFERENCES

- (1) Petrongolo, C.; Buenker, R. J.; Peyerimhoff, S. D. *J. Chem. Phys.* **1982**, *76*, 3655–3667.
- (2) Lindh, R.; Roos, B. O. *Int. J. Quantum Chem.* **1989**, *813*–825.
- (3) Serrano-Andrés, L.; Merchán, M.; Nebot-Gil, I.; Lindh, R.; Roos, B. O. *J. Chem. Phys.* **1993**, *98*, 3151–3162.
- (4) Watts, J. D.; Gwaltney, S. R.; Bartlett, R. J. *J. Chem. Phys.* **1996**, *105*, 6979–6988.
- (5) Finley, J.; Malmqvist, P.-Å.; Roos, B. O.; Serrano-Andrés, L. *Chem. Phys. Lett.* **1998**, *288*, 299–306.
- (6) Davidson, E. R.; Jarzecki, A. A. *Chem. Phys. Lett.* **1998**, *285*, 155–159.
- (7) Müller, T.; Dallos, M.; Lischka, H. *J. Chem. Phys.* **1999**, *110*, 7176–7184.
- (8) Ben-Nun, M.; Martínez, T. J. *Chem. Phys.* **2000**, *259*, 237–248.
- (9) Baek, K. K.; Martínez, T. J. *Chem. Phys. Lett.* **2003**, *375*, 299–308.
- (10) Hazra, A.; Chang, H. H.; Nooijen, M. J. *Chem. Phys.* **2004**, *121*, 2125–2136.
- (11) Schautz, F.; Filippi, C. *J. Chem. Phys.* **2004**, *120*, 10931–10941.
- (12) Schreiber, M.; Silva-Junior, M. R.; Sauer, S. P. A.; Thiel, W. *J. Chem. Phys.* **2008**, *128*, 134110–134124.
- (13) Angeli, C. *J. Comput. Chem.* **2009**, *30*, 1319–1333.
- (14) Shahi, A. R. M.; Cramer, C. J.; Gagliardi, L. *Phys. Chem. Chem. Phys.* **2009**, *11*, 10964–10972.
- (15) Sauri, V.; Serrano-Andrés, L.; Shahi, A. R. M.; Gagliardi, L.; Vancoillie, S.; Pierloot, K. *J. Chem. Theory Comp.* **2011**, *7*, 153–168.
- (16) Cave, R. J.; Davidson, E. R. *Chem. Phys. Lett.* **1988**, *148*, 190–196.
- (17) Cronstrand, P.; Christiansen, P.; Norman, P.; Agren, H. *Phys. Chem. Chem. Phys.* **2001**, *3*, 2567–2575.
- (18) Ostojić, B.; Domcke, W. *Chem. Phys.* **2001**, *269*, 1–10.
- (19) Boggio-Pasqua, M.; Bearpark, M. J.; Klene, M.; Robb, M. A. *J. Chem. Phys.* **2004**, *120*, 7849–7860.
- (20) Dallos, M.; Lischka, H. *Theor. Chem. Acc.* **2004**, *112*, 16–26.
- (21) Saha, B.; Ehara, M.; Nakatsuji, H. *J. Chem. Phys.* **2006**, *125*, 014316–014329.
- (22) Lehtonen, O.; Sundholm, D.; Send, R.; Johansson, M. P. *J. Chem. Phys.* **2009**, *131*, 024301–024313.
- (23) Send, R.; Sundholm, D.; Johansson, M. P.; Pawłowski, F. *J. Chem. Theory Comp.* **2009**, *5*, 2401–2414.
- (24) Li, X.; Paldus, J. *J. Chem. Phys.* **2011**, *134*, 214118–214132.
- (25) Wilkinson, P. G.; Mulliken, R. S. *J. Chem. Phys.* **1955**, *23*, 1895–1907.
- (26) Mulliken, R. S. *J. Chem. Phys.* **1976**, *66*, 2448–2451.
- (27) Ryu, J.-S.; Hudson, B. S. *Chem. Phys. Lett.* **1995**, *245*, 448–454.
- (28) McDiarmid, R. J. *Chem. Phys.* **1976**, *64*, 514–521.
- (29) Mosher, O. A.; Flicker, W. M.; Kuppermann, A. *J. Chem. Phys.* **1973**, *59*, 6502–6511.
- (30) Doering, J. P.; McDiarmid, R. J. *Chem. Phys.* **1980**, *73*, 3617–3624.
- (31) Booth, G. H.; Thom, A. J. W.; Alavi, A. *J. Chem. Phys.* **2009**, *131*, 054106–054115.
- (32) Cleland, D.; Booth, G. H.; Alavi, A. *J. Chem. Phys.* **2010**, *132*, 041103–041106.
- (33) Booth, G. H.; Alavi, A. *J. Chem. Phys.* **2010**, *132*, 174104–174110.
- (34) Cleland, D.; Booth, G. H.; Alavi, A. *J. Chem. Phys.* **2011**, *134*, 024112–024120.
- (35) Booth, G. H.; Cleland, D.; Thom, A. J. W.; Alavi, A. *J. Chem. Phys.* **2011**, *135*, 084104–084117.
- (36) Rossi, E.; Bendazzoli, G. L.; Evangelisti, S.; Maynau, D. *Chem. Phys. Lett.* **1999**, *310*, 530–536.
- (37) Spencer, J. S.; Blunt, N. S.; Foulkes, W. M. C. *J. Chem. Phys.* **2012**, *136*, 054110–054119.
- (38) Shao, Y.; Molnar, L. F.; Jung, Y.; Kussmann, J.; Ochsenfeld, C.; Brown, S. T.; Gilbert, A. T.; Slipchenko, L. V.; Levchenko, S. V.; O'Neill, D. P.; DiStasio, R. A., Jr.; Lochan, R. C.; Wang, T.; Beran, G. J.; Besley, N. A.; Herbert, J. M.; Yeh Lin, C.; Van Voorhis, T.; Hung Chien, S.; Sodt, A.; Steele, R. P.; Rassolov, V. A.; Maslen, P. E.; Korambath, P. P.; Adamson, R. D.; Austin, B.; Baker, J.; Byrd, E. F. C.; Dachselt, H.; Doerksen, R. J.; Dreuw, A.; Dunietz, B. D.; Dutoi, A. D.; Furlani, T. R.; Gwaltney, S. R.; Heyden, A.; Hirata, S.; Hsu, C.-P.; Kedziora, G.; Khalliulin, R. Z.; Klunzinger, P.; Lee, A. M.; Lee, M. S.; Liang, W.; Lotan, I.; Nair, N.; Peters, B.; Proynov, E. I.; Pieniazek, P. A.; Min Rhee, Y.; Ritchie, J.; Rosta, E.; David Sherrill, C.; Simmonett, A. C.; Subotnik, J. E.; Lee Woodcock, H., III; Zhang, W.; Bell, A. T.; Chakraborty, A. K.; Chipman, D. M.; Keil, F. J.; Warshel, A.; Hehre, W. J.; Schaefer, H. F., III; Kong, J.; Krylov, A. I.; Gill, P. M. W.; Head-Gordon, M. *Phys. Chem. Chem. Phys.* **2006**, *8*, 3172–3191.
- (39) Frisch, M. J.; Trucks, G. W.; Schlegel, H. B.; Scuseria, G. E.; Robb, M. A.; Cheeseman, J. R.; Scalmani, G.; Barone, V.; Mennucci, B.; Petersson, G. A.; Nakatsuji, H.; Caricato, M.; Li, X.; Hratchian, H. P.; Izmaylov, A. F.; Bloino, J.; Zheng, G.; Sonnenberg, J. L.; Hada, M.; Ehara, M.; Toyota, K.; Fukuda, R.; Hasegawa, J.; Ishida, M.; Nakajima, T.; Honda, Y.; Kitao, O.; Nakai, H.; Vreven, T.; Montgomery, J. J. A.; Peralta, J. E.; Ogliaro, F.; Bearpark, M.; Heyd, J. J.; Brothers, E.; Kudin, K. N.; Staroverov, V. N.; Kobayashi, R.; Normand, J.; Raghavachari, K.; Rendell, A.; Burant, J. C.; Iyengar, S. S.; Tomasi, J.; Cossi, M.; Rega, N.; Millam, J. M.; Klene, M.; Knox, J. E.; Cross, J. B.; Bakken, V.; Adamo, C.; Jaramillo, J.; Gomperts, R.; Stratmann, R. E.; Yazyev, O.; Austin, A. J.; Cammi, R.; Pomelli, C.; Ochterski, J. W.; Martin, R. L.; Morokuma, K.; Zakrzewski, V. G.; Voth, G. A.; Salvador, P.; Dannenberg, J. J.; Dapprich, S.; Daniels, A. D.; Farkas, Ö.; Foresman, J. B.; Ortiz, J. V.; Cioslowski, J.; Fox, D. J. *Gaussian 09 Revision A.02*; Gaussian Inc.: Wallingford, CT, 2009.
- (40) Aquilante, F.; De Vico, L.; Ferré, N.; Ghigo, G.; Malmqvist, P.-Å.; Neogrády, P.; Pedersen, T. B.; Pitoňák, M.; Reiher, M.; Roos, B. O.; Serrano-Andrés, L.; Urban, M.; Veryazov, V.; Lindh, R. *J. Comput. Chem.* **2010**, *31*, 224–247.
- (41) Olsen, J.; Jørgensen, P. *J. Chem. Phys.* **1985**, *82*, 3235–3264.
- (42) Koch, H.; Jørgensen, P. *J. Chem. Phys.* **1990**, *93*, 3333–3344.
- (43) Purvis, G. D.; Bartlett, R. J. *J. Chem. Phys.* **1982**, *76*, 1910–1918.
- (44) Christiansen, O.; Koch, H.; Jørgensen, P. *J. Chem. Phys.* **1995**, *103*, 7429–7441.
- (45) Koch, H.; Christiansen, O.; Jørgensen, P.; de Merás, A. M. S.; Helgaker, T. *J. Chem. Phys.* **1997**, *106*, 1808–1818.
- (46) DALTON, A Molecular Electronic Structure Program, Release 2.0; 2005. <http://daltonprogram.org/> (accessed July 12, 2012).
- (47) Kowalski, K.; Piecuch, P. *J. Chem. Phys.* **2001**, *115*, 643–651.
- (48) Kucharski, S. A.; Wloch, M.; Musial, M.; Bartlett, R. J. *J. Chem. Phys.* **2001**, *115*, 8263–8266.
- (49) CFOUR, Coupled-Cluster Techniques for Computational Chemistry, A Quantum-Chemical Program Package by Stanton, J. F.; Gauss, J.; Harding, M. E.; Szalay, P. G. with contributions from Auer, A. A.; Bartlett, R. J.; Benedikt, U.; Berger, C.; Bernholdt, D. E.; Bomble, Y. J.; Cheng, L.; Christiansen, O.; Heckert, M.; Heun, O.; Huber, C.; Jagau, T.-C.; Jonsson, D.; Jusélius, J.; Klein, K.; Lauderdale,

W. J.; Matthews, D.A.; Metzroth, T.; Mück, L. A.; O'Neill, D. P.; Price, D. R.; Prochnow, E.; Puzzarini, C.; Ruud, K.; Schiffmann, F.; Schwalbach, W.; Stopkiewicz, S.; Tajti, A.; Vázquez, J.; Wang, F.; Watts, J. D. and the integral packages MOLECULE (Almlöf, J.; Taylor, P.R.), PROPS (Taylor, P.R.), ABACUS (Helgaker, T.; Jensen, H. J. Aa.; Jørgensen, P.; Olsen, J.;), and ECP routines by Mitin, A. V.; van Wüllen, C.. For the current version, see <http://www.cfour.de> (accessed July 12, 2012).

(50) Dunning, T. H., Jr. *J. Chem. Phys.* **1989**, *90*, 1007–1023.

(51) Widmark, P.-O.; Malmqvist, P.-Å.; Roos, B. O. *Theor. Chim. Acta* **1990**, *77*, 291–306.

(52) We take the diffuse functions from the aug-cc-pVXZ basis sets in the EMSL Basis Set Library. <http://bse.pnl.gov> (accessed July 12, 2012).

(53) Haugen, W.; Trættemberg, M. *Acta Chem. Scand.* **1966**, *20*, 1726–1728.

(54) Kuchitsu, K.; Fukuyama, T.; Morino, Y. *J. Mol. Struct.* **1968**, *1*, 463–479.

(55) Kveseth, K.; Seip, R.; Kohl, D. A. *Acta Chem. Scand., Ser. A* **1980**, *34*, 31–42.

(56) Caminati, W.; Grassi, G.; Bauder, A. *Chem. Phys. Lett.* **1988**, *148*, 13–16.

(57) Herzberg, G. *Electronic Spectra of Polyatomic Molecules*; Van Nostrand: Princeton, 1966.

(58) Duncan, J. L.; Wright, I. J.; Lerberghe, D. V. *J. Mol. Spectrosc.* **1972**, *42*, 463–477.

(59) Craig, N. C.; Groner, P.; McKean, D. C. *J. Phys. Chem. A* **2006**, *110*, 7461–7469.

(60) Langhoff, S. R.; Davidson, E. R. *Int. J. Quantum Chem.* **1974**, *8*, 61–72.